

# LAYER-BY-LAYER PATTERN PROPAGATION AND PULSED LASER DEPOSITION

F. WESTERHOFF, L. BRENDEL, D.E. WOLF

*Gerhard-Mercator-Universität Duisburg, 47048 Duisburg*

In this article kinetic Monte Carlo simulations for molecular beam epitaxy (MBE) and pulsed laser deposition (PLD) are compared. It will be shown that an optimal pattern conservation during MBE is achieved for a specific ratio of diffusion to deposition rate. Further on pulsed laser deposition is presented as an alternative way to control layer by layer growth. First results concerning the island density in the submonolayer regime are shown.

## 1 Introduction

Multi-layered structures with sharp interfaces are of high interest, due to the new physical properties they exhibit resulting from the reduced dimensionality. In order to obtain such sharp interfaces the deposited material has to grow in layers instead of forming 3D islands. Two different methods of growing thin films will be compared here.

Molecular beam epitaxy (MBE) allows to produce mono-crystalline layer structures with high sharpness at the interfaces. Growth takes place in an ultra high vacuum chamber in which the material is thermally evaporated and thus is deposited on the substrate with a continuous flux  $F$ .

The fabrication of thin films with pulsed laser deposition (PLD) is a quite new technique which can improve layer by layer growth.<sup>1</sup> In addition PLD provides the possibility to deposit any desired material with the stoichiometry of the ablated material being conserved. In contrast to thermal evaporation in MBE many particles are ablated from the target simultaneously, resulting in a high adatom density directly after the pulse. This causes an increased islands density in the PLD as will be described.

## 2 Molecular Beam Epitaxy

For an initially flat surface layer by layer growth usually improves, the higher the temperature of the substrate is.<sup>2</sup> But a pattern (e.g. a structure produced by lithographic techniques) will in general not be conserved better during layer by layer growth, if the substrate temperature is raised. The reason is, that for high temperatures the adatoms do not nucleate on top of the islands any more because the diffusion length becomes too large. Instead they are

incorporated at the edges of the islands and therefore flatten the surface which means that information about the pattern gets lost. As the diffusion length depends on the ratio of the diffusion rate to the deposition rate,<sup>3</sup> this value has to be optimized if a given pattern should be conserved during growth. One can also consider the opposite optimization problem: How to choose the growth parameters in order to heal any unwanted structures as efficiently as possible? As the two optimization problems are obviously two sides of the same medal, we consider only the first one in the following.

### 2.1 Model

In the simulation we use a simple cubic crystal with periodic boundary conditions and assume that growth takes place without overhangs and defects. The size of the substrate is  $(L \cdot a)^2$ ,  $L^2$  denoting the number of lattice sites and  $a$  the lattice constant. The atoms are deposited with a flux  $F$  and diffuse with the diffusion constant  $D$  until they are irreversibly bound to another adatom or an island edge.

By *pattern propagation* we mean the deterministic height increase by one lattice constant during the deposition of one monolayer. The probability for pattern propagation<sup>4</sup> is then the fraction of sites which were conserved in every monolayer until time  $t$ :

$$p(t) = \left\langle \prod_{s=1}^t \delta_{h(\vec{x},s),h(\vec{x},s-1)+1} \right\rangle \quad (1)$$

### 2.2 Results

Figure 1 (a) shows  $p(t)$  for an initially flat surface. The exponential decay  $p(t) = \exp(-t/t_c)$  is what one would expect, if the propagation of the surface sites from one layer to the next would be temporally uncorrelated with constant transition probability  $p(1)$ . Surprisingly, the exponential decay of  $p(t)$  is found although there is clear evidence that transition probabilities are temporally correlated.<sup>5</sup> The *life time*  $t_c$  (Fig. 1 b) of the initial surface configuration is determined from the slope of  $\ln(p(t))$ . The data give a power law for  $t_c$  extending over 6 decades:

$$t_c \propto (D/F)^{0.20 \pm 0.01} \quad (2)$$

In the limit of  $D/F \rightarrow 0$  (random deposition) we get  $t_c = 1$ .<sup>6</sup> That the last data point in Fig.1 (b) deviates from the power law is a finite size effect.

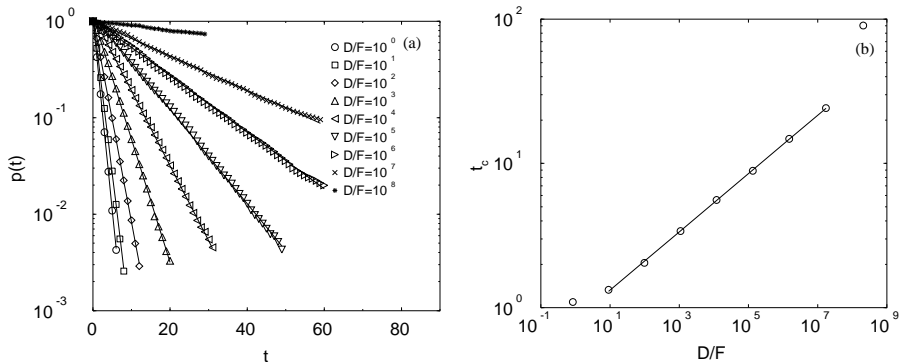


Figure 1. (a) Propagation for an initially flat surface. (b) Life time  $t_c(D/F)$ .

In a study of the one dimensional case<sup>4,6</sup> a logarithmic dependence ( $t_c \sim \log(D/F)$ ) was found. Most recent calculations seem to show a cross over from power law to logarithmic dependence for larger  $D/F$  in two dimensions, as well.<sup>7</sup>

### 2.3 Structured surfaces

As long as the pattern is large compared to the diffusion length for an initially flat surface, the propagation probability should not change since the adatoms will not notice the pattern during their life time. Therefore we also expect an exponential decay for small ratios of  $D/F$ . Here we consider larger values for  $D/F$ , though, where we observe a different behavior. We find a maximum in  $t_c(D/F)$  which is shifted to higher  $D/F$  with growing pattern size  $r$  (Fig. 2 a). This can be explained by the existence of two different mechanisms responsible for the pattern's decay.

For small  $D/F$  the life time  $t_c$  is independent of the island size. This is the regime where the pattern vanishes through kinetic roughening. To the right of the maximum the diffusion length  $l_D$  is large compared to the pattern size, hence there are almost no nucleations on top of the “artificial” islands. Instead, they take on the form of natural growing and coalescing islands. In this way the pattern is also lost.

We find (see Fig.2 b) that the maximum life time  $t_{c,\max}$  for a given pattern length scale  $r$  is reached for

$$(D/F)_{\max} \propto r^{2.4 \pm 0.1} \quad \text{and scales like} \quad t_{c,\max} \propto r^{0.50 \pm 0.05}. \quad (3)$$

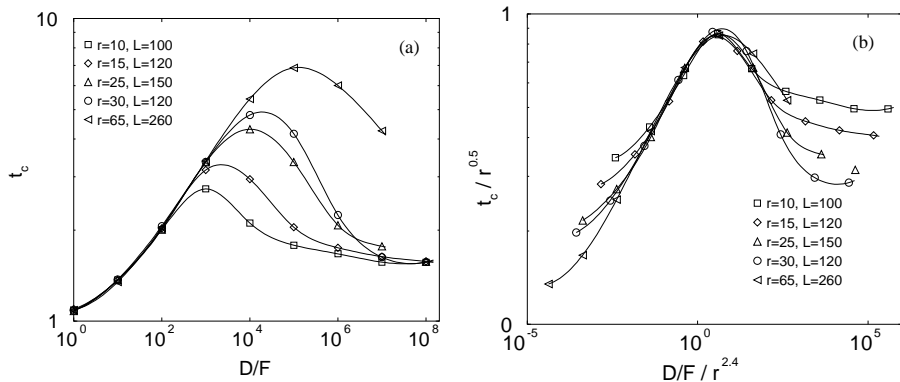


Figure 2. (a) Life time  $t_c$  for patterned surfaces. (b) Scaled data.

This is in agreement with (2):  $t_{c,\max} \propto (D/F)_{\max}^{0.5/2.4} = (D/F)_{\max}^{0.21}$ . As (2) crosses over to a much weaker dependence for very large  $D/F$ , we expect also that (3) will be modified for larger  $r$ .

### 3 Pulsed laser deposition

In pulsed laser deposition the atoms are deposited with a pulse intensity  $I$  (number of atoms per unit area) and frequency  $\omega$  forming an effective (average) flux

$$F = I \cdot \omega. \quad (4)$$

If we reduce the intensity  $I$  to the limiting case of one atom per pulse and at the same time increase the frequency so that the effective flux stays constant, we will reach conditions equivalent to thermal deposition (MBE).<sup>a</sup> One should therefore expect that both methods show similar characteristics in the submonolayer regime.

If the intensity is increased, one should expect a higher island density, because the adatom density and therefore the probability for nucleation is also larger. Hence we predict a *critical pulse intensity*  $I_c$  which separates both regimes.

In the simulation the kinetic energy of the arriving atoms is neglected. This should be a valid approximation for experiments, in which the laser

<sup>a</sup>Nevertheless in the simulation there is still a small difference since in PLD atoms are deposited at fixed time intervals, whereas in MBE fluctuations may occur.

intensity is just above the ablation threshold<sup>1</sup> or the deposition takes place, e.g. in an oxygen atmosphere which slows down the arriving particles.

### 3.1 Critical pulse intensity

During thermal deposition the time evolution of the adatom density  $\rho$  is given by a gain term, the flux  $F$  and a loss term  $\rho/\tau$ , where  $\tau$  is the life time of adatoms on the surface:

$$\dot{\rho} = F - \frac{\rho}{\tau}. \quad (5)$$

In the quasistationary regime (after island nucleation and before island coalescence) the life time  $\tau$  is determined by the typical distance  $l_D$  an adatom diffuses before reaching an island edge<sup>8</sup>:  $\tau = l_D^2/D$ . Then  $\dot{\rho}$  can be neglected and one gets:

$$\rho \approx F \cdot \tau = F \cdot \frac{l_D^2}{D}. \quad (6)$$

With  $l_D \propto \left(\frac{D}{F}\right)^\gamma$  and  $\gamma = 1/6$  for two dimensions and irreversible aggregation<sup>3</sup> this leads to

$$\rho \propto l_D^{-4}. \quad (7)$$

Equation (7) describes the adatom density for thermal deposition. In PLD with a pulse intensity  $I$  much smaller than this density, the adatom density will oscillate around this value with the frequency  $\omega$ . Then one expects the same scaling of the island density as for thermal deposition. By contrast a much larger pulse intensity would prevent the adatom density in PLD to become on average similar to the one in MBE. Hence the critical pulse intensity is expected to be of the order

$$I_c \propto l_D^{-4} \propto \left(\frac{D}{F}\right)^{-2/3}. \quad (8)$$

In the case of a large pulse intensity, the island density increases to such a degree that the life time of the adatoms is shorter than the time between two pulses. Hence the adatom density and therefore the island density becomes independent of the pulse frequency and only depends on  $I$ .

### 3.2 Results

Fig. 3 (a) depicts the island density as a function of the deposited monolayers. We expect three different regimes<sup>9</sup>: The regime for the nucleation of islands,

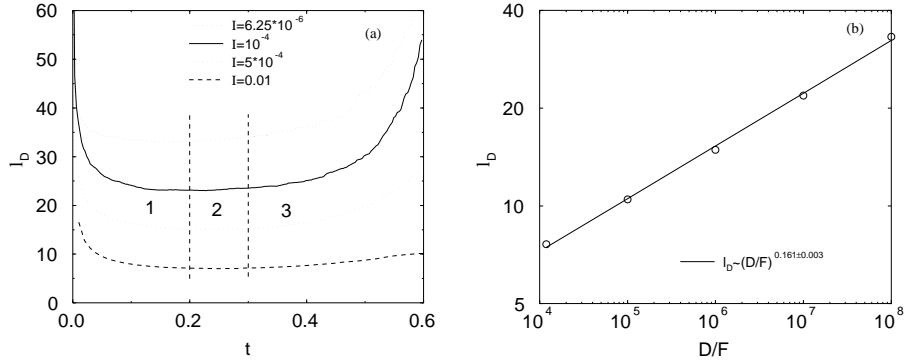


Figure 3. (a) Island distance  $l_D$  as a function of time  $t$  (in units of monolayers). (b)  $l_D(D/F)$  for the limiting case of one atom per pulse.

the saturation of the island density and finally the coalescence of islands with an increasing island distance. An increase of the pulse intensity leads to an overall decrease of the island distance.

### 3.3 $l_D$ for the limit of small pulse intensities

According to a classical result, confirmed by experiments<sup>10</sup> and simulations<sup>9,11</sup> the island distance scales like:

$$l_D \propto \left(\frac{D}{F}\right)^{1/6} \quad (9)$$

This behavior is confirmed in figure 3 (b) for the limit, that only one atom per pulse ( $I \cdot L^2 \rightarrow 1$ ) is deposited.

### 3.4 Scaling behavior of the island distance

Figure 4 (a) depicts the island distance  $l_D$  as a function of the pulse intensity  $I$ . For small values of  $I$  the diffusion length approaches a constant value, which is the island distance for the MBE case. For larger pulse intensities  $l_D$  is described by a power law:

$$l_D \propto I^{-\nu}. \quad (10)$$

It turns out that  $l_D$  can be written in a scaling form:

$$l_D \propto \left(\frac{D}{F}\right)^\gamma \cdot f\left(\frac{I}{I_c}\right) \quad (11)$$

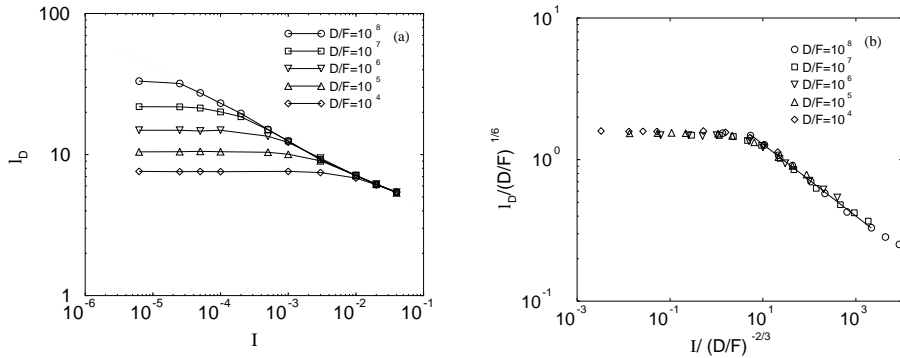


Figure 4. (a) Island distance as a function of the pulse intensity for different ratios of  $D/F$ . (b) Scaled data.

with

$$f(y) \begin{cases} = \text{const.} & \text{for } y \ll 1 \text{ and} \\ \sim y^{-\nu} & \text{for } y \gg 1. \end{cases} \quad (12)$$

While the asymptotic power laws (9,10) were also obtained by Jensen and Niemeyer<sup>12</sup>, the scaling law (11) is new. In the previous work the pulses had a finite duration in contrast to the case presented here. This additional characteristic time spoiled the scaling.

Since for large  $I$ , the  $\omega$ -dependence (via F (4)) has to vanish:

$$I_c^\nu \cdot \left(\frac{D}{F}\right)^\gamma = \text{const.} \quad (13)$$

and therefore:

$$I_c \propto \left(\frac{D}{F}\right)^{-\gamma/\nu} \quad (14)$$

For large pulse intensities we find in Fig. 4 (a) the slope  $\nu = 0.248$ , so that, together with  $\gamma = 1/6$ , we get:

$$\gamma/\nu \approx 2/3,$$

in accordance with the theoretical prediction (8).

## Acknowledgments

We thank the Neumann Institute of Computing (NIC) in Jülich for providing computer time on the CRAY T3E for this project.

## References

1. H. Jenniches, M. Klaua, H. Höchle, J. Kirschner, *Appl. Phys. Lett.* **69**, 3339 (1996).
2. H. Kallabis, L. Brendel, J. Krug, D. E. Wolf, *Int. J. Mod. Phys. B* **11**, 3621 (1997).
3. D. E. Wolf, *Adatom Diffusion and Epitaxial Growth*, in: *Dynamics of Fluctuating Interfaces and Related Phenomena* (World Scientific, Singapore, 1997).
4. H. Kallabis, D. E. Wolf, *Phys. Rev. Lett.* **79**, 4854 (1997).
5. F. Westerhoff, *Musterpropagation im Lagenwachstum* (diploma thesis, Duisburg, 1998).
6. Harald Kallabis, *Theoretical Aspects of Crystal Growth* (Ph. D. thesis, Jülich, 1997).
7. F. Westerhoff, L. Brendel, S. B. Lee, D. E. Wolf, to be published
8. J. Villain, A. Pimpinelli, L.-H. Tang, D. E. Wolf; *J. Phys. I France* **2**, 2107 (1992)
9. L.-H. Thang, *J. Phys. I France* **3**, 935 (1993).
10. S. Günther, E. Kopatzki, M. C. Bartelt, J. W. Evans, R. J. Behm, *Phys. Rev. Lett.* **73**, 553 (1994).
11. S. Stoyanov, D. Kashchiev in *Current Topics in Material Science* **7**, 69, ed. E. Kaldis (North-Holland, Amsterdam, 1981).
12. P. Jensen, B. Niemeyer, *Surf. Sci.* **384**, L823 (1997)